JOURNAL OF Materials CHEMISTRY

Synthesis and photoelectrochemical properties of a fullerene–azothiophene dyad

Sandro Cattarin,[a] Paola Ceroni,[b] Dirk M. Guldi,[c] Michele Maggini,*[d] Enzo Menna,[d] Francesco Paolucci,[b] Sergio Roffia[b] and Gianfranco Scorrano[d]

[a]*Istituto di Polarografia ed Elettrochimica Preparativa-C.N.R., Corso Stati Uniti 4, 35127 Padova, Italy*
[b]*Dipartimento di Chimica «G. Ciamician», Università di Bologna, Via Selmi 2, 40126 Bologna, Italy*
[c]*Radiation Laboratory, University of Notre Dame, Notre Dame, IN 46656, USA*
[d]*CMRO-CNR, Dipartimento di Chimica Organica, Università di Padova, Via Marzolo 1, 35131 Padova, Italy. E-mail: maggini@mail.chor.unipd.it*

Received 1st July 1999, Accepted 6th September 1999

In this paper we describe the synthesis, electrochemistry and photophysical behavior of a fullerene-based donor–acceptor dyad (**2**) in which the donor unit is an azothiophene dye. Dyad **2**, prepared in one step starting from C_{60}, commercially available *N*-methylglycine and thienylazobenzeneamine **1**, can be selectively excited in the visible region where the dye has an absorption maximum at 567 nm. Implementation of electrochemical and photophysical data reveals that both intramolecular energy- and electron-transfer are thermodynamically feasible processes. Steady-state luminescence of dyad **2** in CH_2Cl_2 shows a quenching of the dye singlet excited state (^{1}dye*) and evidence of the fullerene singlet excited state ($^1C_{60}$*) emission. Flash-photolytic experiments, on the other hand, exhibit characteristic differential absorption changes attributed to the $C_{60}^{\cdot -}$–dye$^{\cdot +}$ charge-separated state. Interestingly, it has been estimated that the energy difference between $^1C_{60}$* and the charge separated state is very small, leading to the hypothesis that a rapid exchange between the two states occurs. Sensitization of TiO_2 with dyad **2** and model compound **3** is also reported and discussed.

Introduction

The covalent functionalization of the fullerenes has developed rapidly in the last few years to the extent that now C_{60}, which is by far the most studied fullerene, can be considered a versatile building block in organic chemistry.[1] Major advances in the understanding of the basic principles of C_{60} chemical reactivity gave rise to a large number of functionalized fullerenes that have been tested as active components for biological applications[2] and as new materials.[3] The unique size and symmetry of its delocalized π-electron system makes C_{60} a good electron acceptor both in the ground and excited states.[4]

In this context, a variety of elaborate C_{60}-based donor–acceptor dyads, and higher order photo- and/or electro-active assemblies,[5] have been designed and studied. The fundamental understanding of their photophysical properties helps to shed light onto factors that govern energy and electron transfer processes in relation to natural photosynthesis and to practical applications such as photovoltaic devices for solar energy conversion.[6]

In this connection, we report here the synthesis, electrochemistry and photophysical behavior of the fullerene–azothiophene hybrid **2**[7] and preliminary data on its utilization as sensitizer for mesoporous TiO_2.[8–11]

Experimental

General

Absorption spectra were recorded with a Perkin-Elmer λ6 spectrophotometer. Emission and excitation spectra were obtained with a Perkin-Elmer LS50 spectrofluorimeter. Estimated experimental uncertainties are: $\lambda_{abs} = \pm 2$ nm and $\lambda_{em} = \pm 5$ nm. Details regarding the instrumentation used in this work to characterize compounds **2** and **3**,[12] and to perform flash-photolytic and pulse-radiolytic experiments[13] have been reported elsewhere.

Abbreviations

AcOEt, ethyl acetate; THF, tetrahydrofuran; TBAH, tetrabutylammonium hexafluorophosphate; CV, cyclic voltammetry; SCE, standard calomel electrode; NHE, normal hydrogen electrode; EC, electrochemical chemical; ED, electron donating; EW, electron withdrawing; NIR, near infrared; ITO, indium–tin oxide; IPCE, incident photon-to-current conversion efficiency.

Materials

C_{60} was purchased from Bucky USA (99.5%). *N*,*N*-Diethyl-3-acetamido-4-[(5-formyl-4-chloro-3-cyano-2-thienyl)azo]benzeneamine **1** was a gift from BASF-AG, Ludwigshafen, Germany. All other reagents were used as purchased from Fluka and Aldrich. *N*-Methylfulleropyrrolidine **4** was prepared as described in the literature.[14] Toluene, dichloromethane, acetonitrile, acetone and propan-2-ol, employed for UV–Vis, fluorescence, phosphorescence, pico- and nanosecond flash photolysis, and pulse radiolysis measurements, were commercial spectrophotometric grade solvents that were carefully deoxygenated prior to use. TBAH was used, in the electrochemical experiments, as received. The solvents for CV measurements were prepared as follows: dry vacuum-distilled THF was mixed under argon with sodium anthracenide and allowed to stand for 6–7 days in order to remove traces of water and oxygen whereas dry vacuum-distilled CH_2Cl_2 was stored for several days under argon over 4 Å molecular sieves, activated at 350 °C. Traces of oxygen were removed by

performing several freeze–thaw–pumping cycles. The solvents were then distilled into the electrochemical cell soon before performing the experiment. Solutions for photoelectrochemical measurements (0.2 M $LiClO_4$ and 0.2 M NaI, adjusted to pH = 3 with diluted $HClO_4$) were prepared using water deionized by a Millipore Milli-RO system ($\rho > 5$ MΩ cm) and during experiments were maintained under a nitrogen stream. Layers of commercial nanocrystalline TiO_2 powder (Degussa P25) were deposited on ITO-coated glass samples according to the procedure described in detail by Grätzel and co-workers.[15]

Syntheses

Fulleropyrrolidine 2. A solution of C_{60} (360 mg, 0.5 mmol), **1** (200 mg, 0.5 mmol) and *N*-methylglycine (90 mg, 1.0 mmol) in chlorobenzene (200 mL) was heated to reflux for 2 h. The solvent was evaporated under reduced pressure and the crude product purified by flash column chromatography (SiO_2). Elution with toluene then toluene–AcOEt 95 : 5 gave **2** (184 mg, 32%) along with unreacted C_{60} (219 mg, 61%). IR (KBr): $\nu = 2925$, 2783, 2220, 1614, 1321, 1260, 527 cm^{-1}; ^1H NMR (CD_2Cl_2–CS_2 2 : 1) δ 1.35 (t, 6H), 2.30 (s, 3H), 2.96 (t, 3H), 3.58 (q, 4H), 4.38 (d, 1H), 5.02 (d, 1H), 5.59 (s, 1H), 6.57 (broad m, 1H), 7.61 (broad m, 1H), 8.29 (broad m, 1H). The low solubility of **2** produced a concomitant low signal to noise ratio in the ^{13}C NMR spectrum that hampered a precise analysis of the closely overlapping host of resonances in the aromatic region. Therefore, only the resonances relative to aliphatic carbons are given. ^{13}C NMR (CD_2Cl_2–CS_2 2 : 1) δ 12.8, 29.8, 40.2, 45.5, 69.6. MS (MALDI): $m/z = 720$ $[C_{60}]^+$, 1150 $[M]^+$, 1173 $[M+Na]^+$, 1189 $[M+K]^+$. $C_{80}H_{23}N_6OClS$ (1150): calcd. C 83.44, H 2.01, N 7.30, S 2.78; found C 81.82, H 1.92, N 7.00, S 2.81%. Although the value for carbon is low, it is not unusual for fullerene derivatives.[16]

***N*,*N*-Diethyl-3-acetamido-4-[(5-hydroxymethyl-4-chloro-3-cyano-2-thienyl)azo]benzeneamine 3.** To a solution of aldehyde **1** (400 mg, 0.99 mmol) in EtOH (400 ml) $NaBH_4$ (40.5 mg, 1.05 mmol) in EtOH (50 ml) was added dropwise over a period of 30 min. During the addition, the color progressively changed from deep blue to purple. When the addition was complete, the mixture was brought to reflux and stirred for 3 h. The solvent was evaporated under reduced pressure and the crude product purified by flash column chromatography (SiO_2). Elution with toluene–AcOEt 95 : 5 and then 85 : 15 gave **3** (254 mg, 63%), R_f (toluene–AcOEt 9 : 1) = 0.16. IR (KBr) $\nu = 3412$, 2958, 2924, 2853, 2222, 1620, 1533, 1328, 1150 cm^{-1}; ^1H NMR ($CDCl_3$) δ 1.29 (t, 6H), 2.33 (s, 3H), 3.53 (q, 4H), 4.78 (s, 2H), 6.51 (dd, 1H, $J = 9.3$ Hz, $J = 2.9$ Hz), 7.6 (broad m, 1H), 8.15 (broad m, 1H); ^{13}C NMR ($CDCl_3$) δ 25.9, 30.1, 45.6, 58.1, 100.9, 108.3, 113.3, 130.1, 135.0, 153.5, 166.2. $C_{18}H_{20}N_5O_2ClS$ (405): calcd. C 53.32, H 4.98, N 17.28, S 7.89; found C 53.94, H 5.14, N 17.87, S 7.90%.

Electrochemical and photoelectrochemical instrumentation and measurements

The one-compartment electrochemical cell was of airtight design with high-vacuum glass stopcocks fitted with either Teflon or Kalrez (DuPont) O-rings in order to prevent contamination by grease. The connections to the high-vacuum line and to the Schlenk containing the solvent were obtained by spherical joints also fitted with Kalrez O-rings. The pressure measured in the electrochemical cell prior to performing the trap-to-trap distillation of the solvent was typically $2.0–3.0 \times 10^{-5}$ mbar. The working electrode was a 0.6 mm-diameter platinum wire (approximately 0.15 cm^2) sealed in glass. The counter electrode consisted of a platinum spiral and the quasi-reference electrode was a silver spiral. The quasi-reference electrode drift was negligible for the time required by a single experiment. Both the counter and the reference electrode were separated from the working electrode by ~ 0.5 cm. Potentials were measured with the ferrocene standard and were always referred to SCE. $E_{1/2}$ values correspond to $(E_{pc} + E_{pa})/2$ from CV. Ferrocene was also used as an internal standard for checking the electrochemical reversibility of a redox couple. The temperature dependence of the ferrocenium/ferrocene couple standard potential was measured with respect to SCE by a non-isothermal arrangement according to a reported procedure.[17]

Voltammograms were recorded with an AMEL Model 552 potentiostat controlled by either an AMEL Model 568 function generator or an ELCHEMA Model FG-206F. Data acquisition was performed by a Nicolet Mod 3091 digital oscilloscope interfaced to a PC. Temperature control was accomplished within 0.1 °C with a Lauda Klein-Kryomat thermostat.

Photoelectrochemical experiments were carried out under N_2 atmosphere in a three electrode configuration of a single compartment glass cell equipped with a quartz optical flat. A saturated calomel electrode (SCE) inserted in a side arm and connected to the main compartment by a Luggin capillary was used as reference. All potentials are given *versus* SCE. A standard setup was used: 150 W Xe lamp; monochromator (Applied Photophysics); filters (Schott); light chopper (EG&G Brookdeal model 9479); potentiostat and function generator (Amel models 553 and 568, respectively); lock-in amplifier (PAR model 5210). Monochromatic light power was measured with a calibrated photodiode (Macam Photometrics). Photocurrent spectra were measured under a chopped light (chopping frequencies of 1 to 3 Hz). Conversion efficiency was estimated as the number of electrons flowing in the circuit per photon incident on the working electrode (IPCE)[15,18] without correction for reflection and transmission losses.

Digital simulation of cyclic voltammetric experiments

The CV simulations were carried out using the DigiSim 2.1 software by BAS. The simulation parameters were accurately chosen to obtain a visual best fit over a 10-fold range of scan rates. This procedure allowed the assignment of the rate constants with a 20% error.

Results and discussion

Synthesis

Dyad **2** (Chart 1) was prepared in 32% isolated yield *via* the 1,3-dipolar cycloaddition of azomethine ylides[14,19] to C_{60} by treating *E*-azothiophene aldehyde **1** with *N*-methylglycine and C_{60} in refluxing chlorobenzene. The structure of fulleropyrrolidine **2** was verified by spectroscopic analysis including NMR, MALDI mass spectrum and elemental analysis. Derivatives **3** and **4**[14] have been synthesized and used as model compounds in the electrochemical and photophysical characterization of dyad **2**.

Electrochemistry

Fig. 1a shows the CV curve for a 0.5 mM THF solution of dyad **2**, recorded at 25 °C and at a scan rate of 0.5 V s^{-1}. Six reduction peaks, corresponding to chemically reversible, one-electron redox processes were observed. Peaks I–III and V–VI relate to single Nernstian charge transfer processes whereas peak IV, and its anodic counterpart, relate to a non-Nernstian (quasi-reversible) redox couple.[20]

Measurements at lower temperatures (≤ -30 °C) increased the available potential window allowing the detection of a seventh peak at more negative potentials (not shown). The latter corresponds to a one-electron reduction process with $E_{1/2} \approx -3.0$ V, which partly overlaps the base solution

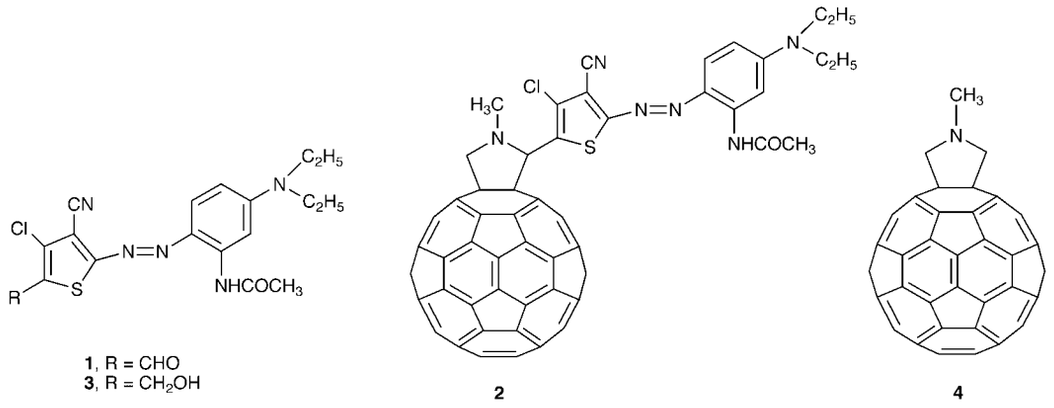

Chart 1

discharge. The $E_{1/2}$ values for dyad **2** and model compounds **3** and **4** are reported in Table 1.

The anodic behavior of dyad **2** was further investigated in CH_2Cl_2. The CV curve, obtained at 25 °C and at a scan rate of 0.5 V s^{-1}, is reported in Fig. 1b. Together with three reduction processes, that are slightly shifted towards more negative potentials if compared to those observed in THF, a single one-electron oxidation process could be detected (Fig. 1b, peak A). Peak A is characterized by partial chemical irreversibility, with a cathodic-to-anodic peak current ratio lower than unity. Within the allowed potential window ($\leqslant$3 V), no further oxidations were observed beyond peak A. However, when the scan rate was increased, and/or the temperature lowered, peak A attained full reversibility with $E_{1/2} = +1.12$ V. This is in line with an EC mechanism where a first-order follow-up reaction is coupled to the electron transfer since no significant effect on the kinetics of the chemical reaction was observed by increasing the concentration of **2**. A rate constant $k = 0.5\ s^{-1}$ (at 25 °C) was obtained by digital simulation of the CV curves based on the above mechanism. The digital simulation of the cathodic CV curve (Fig. 1c) was performed using the experimental $E_{1/2}$ values for all peaks, except peak IV since the corresponding $E_{1/2}$ value cannot be derived from the experimental CV curve. Process IV was simulated using the values of 10^{-3} cm s^{-1} for the heterogeneous charge transfer rate constant, 0.6 for the charge transfer coefficient (α) and $E_{1/2} = -1.44$ V.

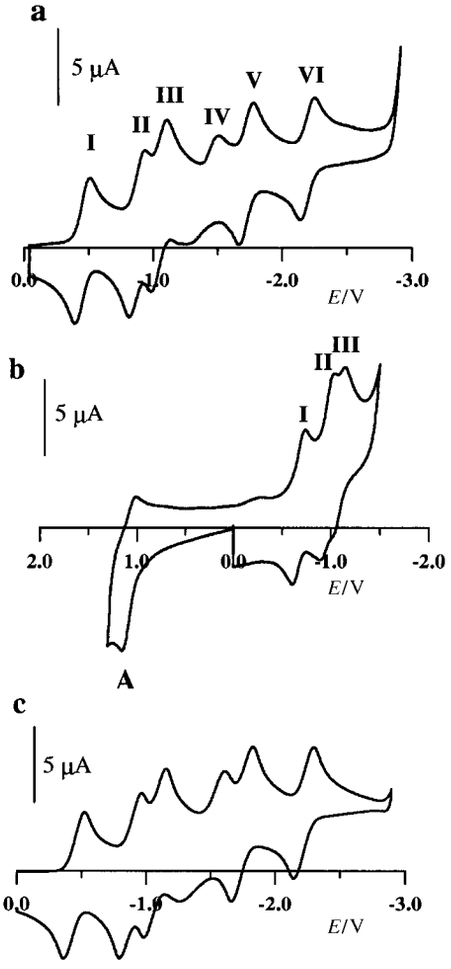

Fig. 1 CV curve of 0.5 mM dyad **2** (0.05 M TBAH, $T = 25$ °C, $v = 0.5$ V s^{-1}) in THF (a) and in CH_2Cl_2 (b). Simulated CV curve (c) under the conditions of (a).

In order to identify the redox sites, and obtain information on their mutual interactions, the electrochemical behavior of **2** was compared with that of *N*-methylfulleropyrrolidine **4** and compound **3**. The similarity of the $E_{1/2}$ values for peaks I, III, V, VI and VII of dyad **2** to the corresponding values for model **4** (apart from a small anticipation in the former) indicates that the above peaks relate to fullerene-centered reductions. The two remaining reductions (II and IV) and the oxidation, not present in **4**, were attributed to redox processes involving the dye moiety by comparison with model compound **3**. In both solvents, two one-electron reduction peaks were observed for **3**. The first reduction corresponds to a Nernstian process, the second to a quasi-reversible process. From the digital simulation of the CV curve, a half-wave potential value of −1.34 V was obtained for the second one-electron reduction, assuming $k_h = 10^{-3}$ cm s^{-1} and $\alpha = 0.6$, in analogy with dyad **2**. The small cathodic shift observed for the dye-based reductions in **2** with respect to **3** (Table 1) can be rationalized in the frame of a simple electrostatic repulsion model since in dyad **2** one or two negative charges are already present on the fullerene moiety during the first and second dye-based reductions. In the anodic region, model compound **3** shows a single oxidation peak superimposable on that observed for dyad **2**.

In accordance with previous work,[21] the processes at −0.88 and −1.34 V were attributed to the reduction of the azo group and the redox potential at +1.12 V to oxidation of the *N*,*N*-diethyl-*m*-acetylamino substituent. It has been shown that azobenzene reductions, located at −1.41 and −1.75 V respectively (acetonitrile–tetraethylammonium perchlorate solutions), are sensitive to substitution on the aromatic rings. In particular, electron-donating (ED) groups shift the azobenzene reductions to the cathodic region, whereas electron-withdrawing (EW) groups shift them to the anodic one. Our push–pull azodye moiety contains competing EW (the substituted thiophene) and ED (the *N*,*N*-diethyl-*m*-acetylamino) units that cause an overall anodic shift of the two reductions of the azo group. This indicates that the EW character of the substituted thiophene prevails over the ED effects of the *N*,*N*-diethyl-*m*-acetylamino group.

Table 1 $E_{1/2}$ values (V *vs.* SCE) of the redox couples of dyad **2** and model compounds **3** and **4**, detected by CV (sweep rate = 0.2 V s^{-1}) in 0.3 mM (0.05 M TBAH) THF or (in brackets) CH_2Cl_2 solutions, at 25 °C[a]

	A	I	II	III	IV	V	VI	VII
2	(+1.12)	−0.45 (−0.64)	−0.88 (−0.93)	−1.06 (−1.1)	−1.44	−1.72	−2.19	−3.0
3	(+1.12)	−0.85 (−0.88)	−1.34 (−1.34)					
4		−0.47 (−0.69)	−1.04 (−1.08)	−1.68	−2.15	−2.96		

[a]Working electrode: Pt; $E_{1/2}^{Fc+/Fc}$ = 0.58 V (THF); 0.46 V (CH_2Cl_2) at 25 °C.

The location of the oxidation process, observed for **2** and **3** at $E_{1/2}$ = 1.12 V, on the thiophene ring is very unlikely. Thiophene, in fact, oxidizes at a potential of 1.4–2.3 V (depending on the substituent)[22] which becomes 0.5–0.7 V more positive when an EW group, such as cyano, is present in the ring.[22] Also the electrochemical oxidation of the azo group should be ruled out. *N*,*N*-Dimethyl-4-aminoazobenzene, for instance, undergoes irreversible oxidation in aqueous solutions at the dimethylamino substituent rather than at the azo group.[21] The $E_{1/2}$ value reported in acetate buffer is 0.93 V[21] which, although referring to quite a different medium, compares well with that relative to the oxidation in **2** and **3**, thus corroborating the attribution that the redox process at +1.12 V refers to oxidation of the *N*,*N*-diethylamino-*m*-acetylaminobenzene part of the chromophore.

Photophysical measurements

Ground-state absorption spectra. The absorption spectra of derivatives **2–4** in CH_2Cl_2 are compared in Fig. 2.

The singlet ground state absorption of **4** lies predominantly in the UV region, as expected for C_{60} and derivatives, while the intense purple-colored solution of model **3** shows its strongest absorption band in the visible region at λ_{max} = 554 nm. Therefore, superimposed features of dyad **2** would enable the selective excitation of the fullerene (UV region) or the dye moiety (visible region). However, the absorption spectrum of **2** is not exactly the sum of the absorptions of **3** and **4**. In fact, a red shifted VIS band from 554 nm (**3**) to 567 nm (**2**) is noted. The red shift either indicates the presence of noticeable electronic interaction between the fullerene and dye moieties in the ground state, in line with the electrochemical analysis, or a differential solvation effect of the two species due to the bulky fullerene moiety hindering approach of solvent to the intrinsically solvatochromic azothiophene chromophore.[23]

Steady-state and time-resolved luminescence. In order to probe the extent of electronic interaction between the two electroactive moieties in the excited state, emission measurements with dyad **2** and models **3** and **4** were carried out in CH_2Cl_2 at 25 °C. Excitation of **3** (λ_{exc} = 538 nm) produces a strong emission band with a maximum around 630 nm (Fig. 3).[24]

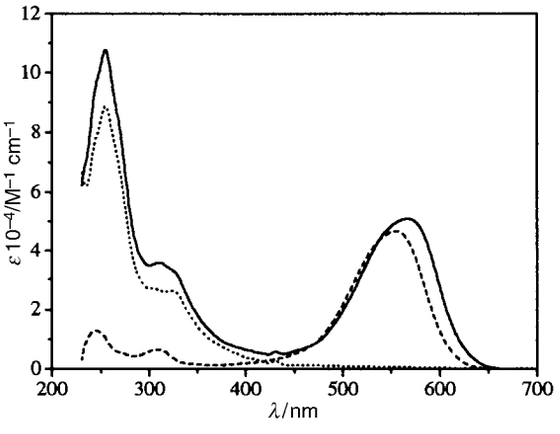

Fig. 2 Absorption spectra for CH_2Cl_2 solutions of **2** (—), **3** (- - - -) and **4** (···).

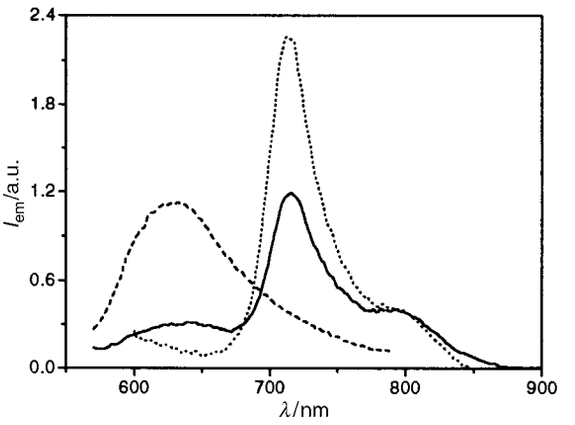

Fig. 3 Emission spectra for CH_2Cl_2 solutions of **2** (—), **3** (- - - -) and **4** (···). λ_{exc} = 538 nm and equal absorbance at 538 nm for **2** and **3**. λ_{exc} = 310 nm for pyrrolidine **4**.

A solution of dyad **2**, with equal absorbance at λ_{exc} = 538 nm, shows the same 630 nm emission as **3**. The fluorescence intensity is, however, remarkably quenched (70%) relative to **3**. More importantly, the emission spectrum gives rise to another band around 716 nm, which corresponds to the fullerene excited singlet state ($^1C_{60}$*) emission of **4**.[25] The quantum yield for the underlying singlet–singlet energy transfer was derived, which amounts, however, only to 50%.

The presence of a fullerene-based emission in dyad **2** and the agreement between absorption and excitation spectra throughout the UV–Vis region suggest that energy transfer is likely to be involved in the deactivation mechanism of the dye singlet excited state. To quantify the deactivation of the ^{1}dye* state we performed, in addition to the steady state emission experiments, a time-resolved emission lifetime measurement. The spectrum of dyad **2** revealed a mono-exponential decay of the dye emission at 630 nm with a lifetime of 58 ps. It should be noted that this value is in excellent agreement with the time-resolved transient absorption experiments (*vide infra*). To get a better insight into the quenching mechanism, time-resolved experiments were performed.

Time-resolved flash photolysis: model compound 3. Picosecond-resolved photolysis of dye **3**, in deoxygenated CH_2Cl_2, led to a strong bleaching of the ground state around 540 nm and grow-in of a new absorption band with a maximum at 635 nm.

Fig. 4a illustrates the above changes between 600 and 750 nm with a 0 ps (before laser irradiation), 125, and 4000 ps time-delay, respectively. The similarity of the spectra recorded 125 and 4000 ps after the laser pulse underlines the stability of the dye singlet excited state on this time scale (*e.g.* picosecond).

Dyad 2. Picosecond-resolved photolysis of a deoxygenated CH_2Cl_2 solution of dyad **2** led to a similar bleaching around 540 nm and a new absorption centered at 635 nm (25 ps after the laser pulse, Fig. 4b). This suggests, in accordance with model **3**, formation of the singlet excited state of the dye moiety. However, the associated decay kinetics differ appre-

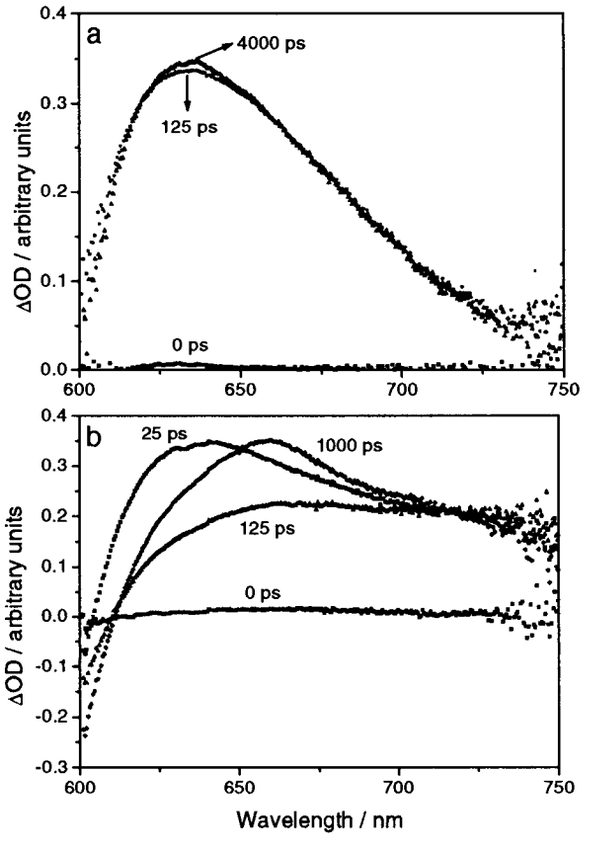

Fig. 4 Time-resolved difference absorption spectra in deoxygenated CH_2Cl_2 solution of (a) dye **3** and (b) dyad **2** (0.02 mM) recorded 0, 125, and 4000 ps after excitation with an 18 ps laser pulse at 532 nm.

ciably from the singlet excited state in model **3** (see kinetic traces, for example, at 600 and 640 nm, Fig. 5). In particular, two quenching components are evident.

The faster quenching is essentially an instantaneous process with $\tau_{1/2} = 65$ ps. The resulting transient, with weak absorption in the Vis-range, is subjected to a second, slower transformation ($\tau_{1/2} = 300$ ps) into a much broader absorbing species. Differential absorption changes recorded with a 125 and 1000 ps time-delay revealed, in the displayed 600–750 nm region, two different products with maxima at 655 and 675 nm, respectively (Fig. 4b), thus corroborating the time evolution.

In view of obtaining direct spectral evidence that would help to identify the transient intermediates, the current measurements were extended to the nanosecond time-regime.

Fig. 6a shows the spectral features of an irradiated CH_2Cl_2 solution of dyad **2** recorded at the end of the picosecond time-scale (6 ns) whereas Fig. 6b displays those monitored immediately after a 20 ns laser pulse (532 nm). Conclusive evidence for involvement of the fullerene radical anion stems from the well-resolved NIR transition around 1060 nm, shown in Fig. 7.

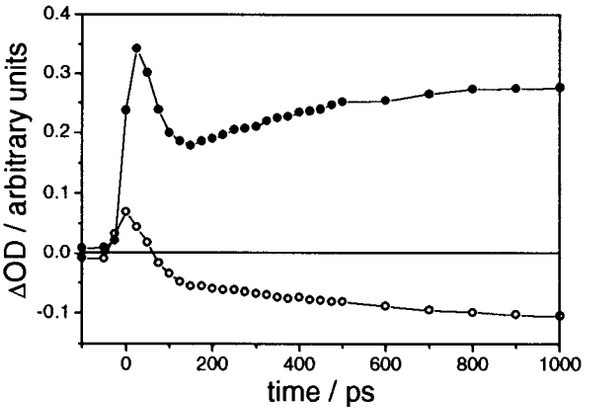

Fig. 5 Time absorption profiles recorded at 600 nm (○) and 640 nm (●) for a deoxygenated CH_2Cl_2 solution of dyad **2** (0.02 mM), following an 18 ps laser pulse at 532 nm.

This suggests interpretation of the observed spectral changes in light of a charge-separated radical pair evolving from an intramolecular electron transfer in photoexcited dyad **2**. The radical pair is, however, short-lived with a lifetime of 84 ns.

Nanosecond photolysis, following the complete decay of the charge separated species, reveals the presence of the fullerene triplet excited state with an overall efficiency of only 6%. It should be noted that the decay of the charge-separated radical pair is not connected to the triplet excited state. The apparent discrepancy between the results of steady-state experiments, in which the singlet–singlet energy transfer to the fullerene accounts for about 50% of the deactivation of the photoexcited dye, and time-resolved photolysis is related to the strong absorption changes in the transient measurements. These make it a difficult task to convolute the singlet–singlet energy transfer pathway. As a consequence, differential absorption changes are dominated by the intramolecular electron transfer event.

In view of the steady-state and time-resolved photophysical experiments, the quenching mechanism of the ^{1}dye* in dyad **2** (1.97 eV) involves both an energy transfer process leading to the $^1C_{60}$* state and an electron transfer, giving the $C_{60}^{\cdot -}$–$dye^{\cdot +}$ charge separated state, as outlined in Scheme 1.

The energy difference between $^1C_{60}$* (1.73 eV) and the charge separated state (1.71 eV, calculated in the frame of the dielectric continuum model[26]) is very small in CH_2Cl_2 leading to the hypothesis that a rapid exchange between the two states occurs. In a parallel experiment, the fullerene moiety, rather than the dye chromophore, was excited with a 337 nm laser pulse and still the overall triplet quantum yield was 0.05, relative to a fullerene standard with an optically matched absorption at 337 nm.[27] Time resolved fluorescence measurements showed, indeed, a rapid quenching of the fullerene singlet excited state emission. In particular, a mono-exponential decay of the 710 nm emission, upon 337 nm excitation, gives rise to a lifetime of 0.6 ns, markedly shorter than that of model compound **1**. The inefficient quenching, despite the close spatial separation of the donor and acceptor moieties, is a further argument that is in support of the small energy gap between the fullerene singlet excited state and the charge-separated state, namely, ($C_{60}^{\cdot -}$–$dye^{\cdot +}$).

Pulse radiolytic reduction and oxidation. In order to further confirm the generation of the reduced fullerene moiety upon photolysis of dyad **2**, pulse irradiation was carried out in a deoxygenated toluene–propan-2-ol–acetone solvent mixture. The radiolysis of this mixture produces the strong reductant $(CH_3)_2{}^{\cdot}C(OH)$. This radical species is either formed *via* electron capture by acetone, followed by a subsequent protonation, or, alternatively, evolves from the direct radiolysis of propan-2-ol. The reduction potential of $(CH_3)_2{}^{\cdot}C(OH)$ in water is −1.63 V. Therefore, this species is expected to transfer an electron to compounds **2** or **4** with less negative first reduction potentials.

UV–Vis differential absorption changes, recorded upon irradiation of a deoxygenated toluene–propan-2-ol–acetone solution of **4** (0.01 mM), showed bleaching of the ground state absorption at 330 nm and a concomitant growth of an absorption at around 400 nm. More importantly, the NIR region revealed an absorption band with λ_{max} at 1010 nm.[28] Since i) radiolysis generates a strongly reducing species which is likely to form the radical anion of **4** and ii) the former bleaching (330 nm) and the latter maximum (1010 nm) are in good agreement with the spectral features recorded upon photo-induced intramolecular quenching of the dye excited state (Fig. 6b and 7), it is reasonable to assume the formation of a charge-separated ($C_{60}^{\cdot -}$–$dye^{\cdot +}$) pair in photoexcited dyad **2**.

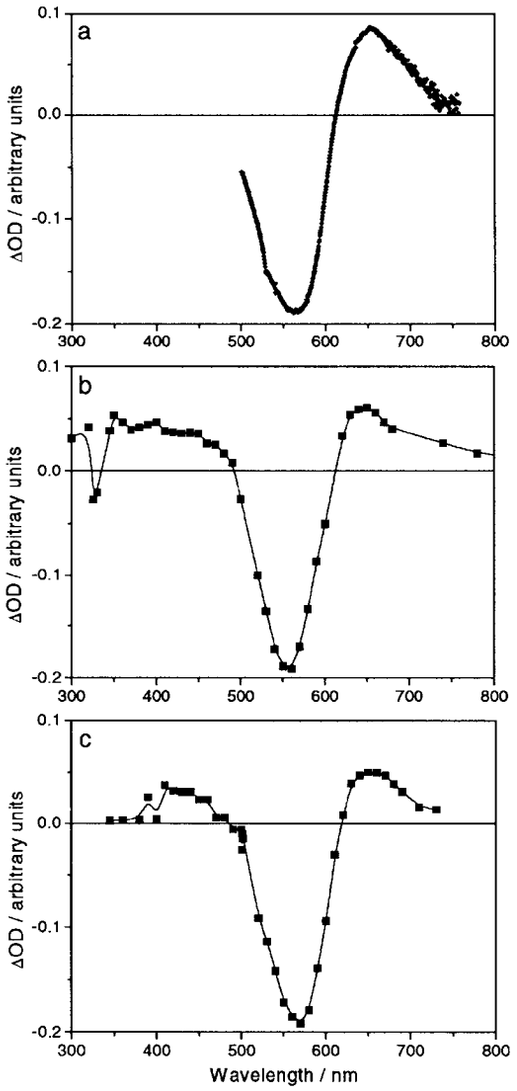

Fig. 6 Transient absorption spectra obtained (a) 4 ns after 18 ps excitation (532 nm) and (b) 20 ns after an 8 ns excitation (532 nm) of dyad **2** (0.02 mM) in deoxygenated CH_2Cl_2. (c) Differential spectrum, upon radiolytic oxidation of **3**, monitored in aerated CH_2Cl_2 solution after completion of the oxidation reaction (100 μs after the pulse).

Radiolytic oxidation of dye **3** was carried out in dilute solutions of aerated CH_2Cl_2. The oxidation reaction involves different radiolytically generated radicals. In particular, **3** is oxidized mainly by $CH_2ClO_2^{\cdot}$ and $CHCl_2O_2^{\cdot}$ radicals, which are formed in the radiolysis of this solvent. It should be noted that a direct oxidation by the solvent radical cation

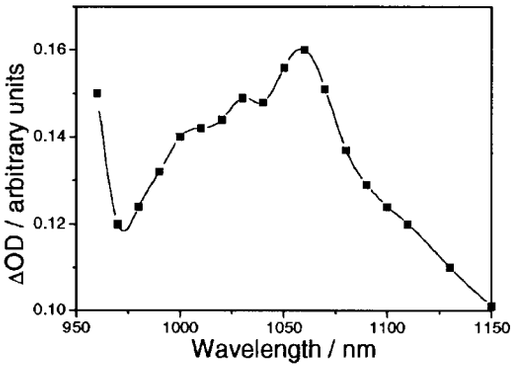

Fig. 7 Differential NIR absorption spectrum obtained upon flash photolysis of dyad **2** (0.02 mM) in CH_2Cl_2 with an 8 ns laser pulse at 532 nm.

($[CH_2Cl_2]^{\cdot+}$) and by Cl atoms, although it may take place, is unimportant since these species are very short-lived and the dye concentration is relatively low.

Pulse radiolysis of **3** resulted in strong bleaching of the starting compound at 560 nm and formation of a broad absorption centered around 650 nm. The spectral changes, shown in Fig. 6c, indicate one-electron oxidation of the dye to its radical cation and are in excellent agreement with the spectral features assigned to the ($C_{60}^{\cdot-}$–$dye^{\cdot+}$) radical pair (Fig. 6a/b).

With the support of pulse radiolysis, we demonstrated that the proposed ($C_{60}^{\cdot-}$–$dye^{\cdot+}$) radical pair exhibits fine structured characteristics. They can be assigned, in part, to the reduced fullerene moiety (bleaching at 330 nm/NIR band at 1010 nm) and to the oxidized dye (bleaching/Vis band around 560 and 650 nm respectively).

Sensitization of TiO_2

The electrochemical and photophysical properties of **2** and **3** make them potential candidates for sensitization of large band-gap semiconductors, such as TiO_2. The redox potential of the dye-centered singlet excited state ($dye^+/^1dye^*$) is *ca.* −0.83 V, based on the dye-centered oxidation $E_{1/2}$ (+1.12 V) and emission λ_{max} (630 nm). This renders the electron injection between interfacial $^1dye^*|TiO_2$ conduction band (CB), located at −0.58 V (aqueous solution, pH = 3), thermodynamically allowed. Scheme 2 shows a plausible energy levels scheme at the TiO_2/adsorbed compound/electrolyte interface, where the adsorption of the dye onto the semiconducting surface is assumed not to bring about significant perturbation of the energy levels.

Quite evidently, intramolecular energy and electron transfer processes occurring in **2** represent competing pathways for the overall deactivation of $^1dye^*$ relative to electron injection into the semiconductor CB. Although such a competition may be significantly biased in favor of the latter process on kinetic grounds,[8] a better performance is in principle expected with **3** rather than **2**. Fullerene singlet and triplet excited states are in fact thermodynamically unable to inject an electron into the semiconductor (the estimated redox potential for $C_{60}^+/^1C_{60}^*$ moiety is +0.54 V, based on C_{60}^+/C_{60} $E_{1/2} = +2.25$ V[29] and C_{60} singlet excited state emission +1.73 eV). Electron injection from a fulleropyrrolidine radical anion is also expected not to occur easily, based on the unfavorable driving force (Scheme 2).

However, attempts to obtain stable coatings of model **3** onto TiO_2 films failed. Although the dye adsorbed from a THF solution, it rapidly deadsorbed under the conditions used for the photoelectrochemical measurements, *e.g.*, aqueous or CH_3CN solutions. This indicates that a physical adsorption is likely to occur rather than a chemisorption as might be expected from the presence of the alcoholic functionality on the thiophene ring. Furthermore, coated TiO_2 films kept in THF solution bleached progressively under daylight illumination,

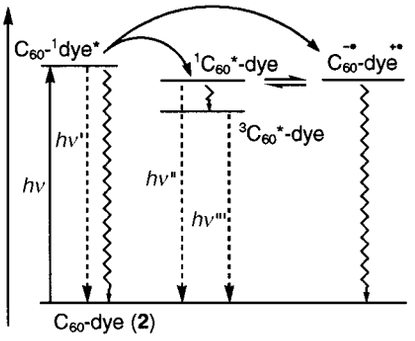

Scheme 1 Energy scheme for the excited states of **2** in CH_2Cl_2. (See text and ref. 26.)

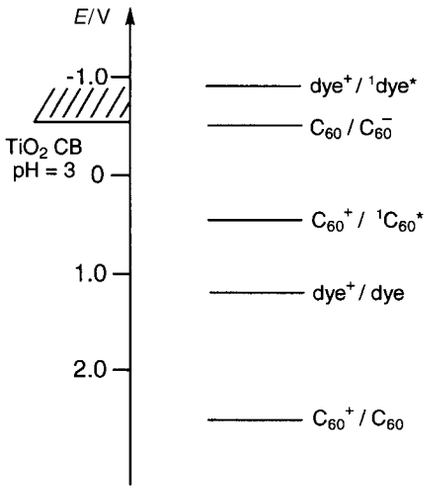

Scheme 2 Plausible energy levels scheme at the TiO_2/adsorbed **2**/electrolyte interface.

indicating significant photodegradation of **3** by TiO_2. This is not totally surprising in view of the well-known ability of TiO_2 to photo-oxidize organic substrates *via* the generation of OH radicals.[30] *Vice versa*, deposition of **2** resulted in photochemically much more stable coatings. For example, after 48 hours of continuous daylight exposure, less than 10% bleaching was observed and no bleaching at all was observed when UV radiation from daylight was filtered off. Since no additional stabilization was proved by the electrochemical investigation for the oxidized dye from the fullerene derivatization, the observed effect was rather attributed to *UV-filtering* exerted by the fullerene moiety in **2**, which prevents much of the UV light from reaching TiO_2 and producing highly energetic holes in the semiconductor. Such effects are absent in **3** due to the much lower extinction coefficient at $\lambda < 350$ nm (compare spectra in Fig. 2). Furthermore, TiO_2 coatings with **2** were found to be very stable in the solution employed for photoelectrochemical experiments. Considering that dyad **2** does not bear functional groups able to covalently link to the TiO_2 surface, the observed high stability can be rationalized in light of the low solubility of **2** (and, in general, of fullerene derivatives) in highly polar solvents. However, interactions of the fullerene moiety with Ti atoms cannot be ruled out, and further work is in progress to elucidate this point.

Photoelectrochemical experiments

Fig. 8 shows two voltammograms recorded in 0.2 M $LiClO_4$, 0.2 M NaI aqueous solution, under illumination with white light from a xenon lamp, using a GG475 long pass filter (Schott) with a cut-on wavelength of 475 nm.

Curve (a) was recorded for bare TiO_2 substrate and curve (b) for a sensitized TiO_2 electrode with dyad **2**. Curve (a) resembles that recorded in the dark, as expected considering that the substrate is not sensitive to wavelengths passing through the filter. Curve (b) shows a significant, although not large, photocurrent indicating sensitization in the visible region of the dye-coated substrate. The region of spectral sensitization is shown by the IPCE spectrum. The IPCE%, namely the fraction of incident photons that 'succeed' in producing electrons in the external circuit, may be expressed as:[31,32]

$$\text{IPCE } \% = \frac{1240}{\lambda \text{ (nm)}} \times \frac{j_{ph} \text{ (mA cm}^{-2})}{\Phi \text{ (mW cm}^{-2})} \times 100$$

where $1240/\lambda$ (nm) is the monochromatic photon energy in eV, j_{ph} the photocurrent density and Φ (mW cm^{-2}) is the light power incident on the (geometric) unitary surface. The IPCE% spectrum is reported in Fig. 9 and shows an extension in the visible region of photocurrent response for the sensitized electrode, well matching the optical spectrum of the sensitizer reported in Fig. 2.

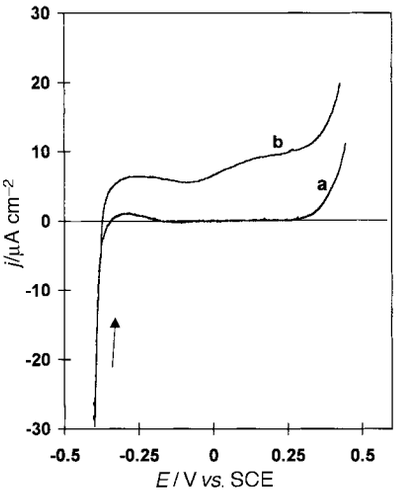

Fig. 8 CV curves recorded at bare (a) and dye-sensitized TiO_2 electrodes (b) illuminated by the light of a Xe lamp filtered through a long pass filter (cut-on wavelength 475 nm). Sweeps were performed from the negative limit in a positive direction (10 mV s^{-1}). Electrolyte: 0.2 M $LiClO_4$, 0.2 M NaI, deaerated by a nitrogen stream.

The process of sensitization is likely to be the same as that already discussed by Grätzel and co-workers.[15,18] In particular, the dye is excited by the incident light producing the excited ^{1}dye* which injects an electron into the conduction band of the semiconductor. The resulting oxidized dye$^+$ is subsequently reduced by a suitable donor in solution regenerating the ground state.

Conclusion

In this paper we have reported the synthesis, electrochemical and photophysical behavior of a donor–acceptor dyad in which C_{60} is covalently linked to a thienylazobenzeneamine derivative. In dyad **2** ground-state interaction occurs between the fullerene and dye units. In fact, the dye electronic absorption is subjected to a red shift from 554 nm (**3**) to 567 nm. Additional evidence for this hypothesis stems from the anticipation of the first fullerene-centered reduction and by the cathodic shift of the dye-based reductions in **2**. However, the electrochemical characterization shows that no additional stabilization of the dye-centered radical cation has been introduced by the presence

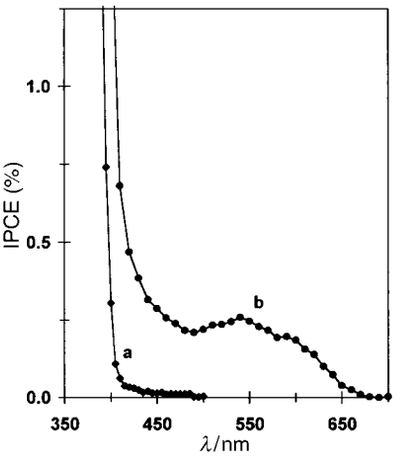

Fig. 9 Steady state IPCE% spectra of a bare (a) and a dye-sensitized nanoporous TiO_2 electrode (b) with back side irradiation (through the ITO substrate). Spectra recorded at the potential $E = 0.35$ V. Same electrolyte as in Fig. 8.

of the covalently linked C_{60}. Complementary emission and transient absorption revealed a rapid deactivation, once photoexcited, of the dye singlet excited state. With the help of radiation chemistry both pathways, namely, a charge separation and singlet–singlet energy transfer were confirmed. An interesting observation is that the energy difference between $^1C_{60}$* and $C_{60}^{\cdot -}$–$dye^{\cdot +}$ is very small, leading to the hypothesis that a rapid exchange between the two states occurs. Finally, we have reported the first example, to our knowledge, of TiO_2 sensitization with a fullerene-based donor–acceptor photoactive dyad. However, observation of a relatively low sensitization suggests that the lifetime of ^{1}dye* is insufficient, decaying to a state thermodynamically unable to inject an electron into the ^{1}dye*|TiO_2 conduction band. Interestingly, the sensitized electrodes were found to be very stable to daylight exposure, if compared to those coated with derivative **3**. This effect has been ascribed to UV-filtering exerted by the fullerene moiety in **2**. Currently, dyads are being produced in which the fullerene is functionalized with a suitable anchoring group, such as silicon trialkoxide, for grafting on the surface of the mesoporous oxide.

Acknowledgements

We are grateful to Dr Thomas Gessner (BASF-AG, Colorant Laboratory, Ludwigshafen, Germany) for calling our attention to derivative **1** and providing a sample. We thank Reza Dadirian Tehrani and Vania Foltran for their help in the development of some of the experimental procedures and Roberta Seraglia (CNR-Padova) for MALDI-MS. Part of this work was supported by Murst (Contract No. 9803194198), by the University of Bologna (funds for selected research topics) and by the Office of Basic Energy Sciences of the U.S. Department of Energy (Contribution No. NDRL-4146 from the Notre Dame Radiation Laboratory). M.M. and D.G. thank NATO for a travel grant (Grant No. CRG960099).

References

1 *Fullerenes and Related Structures*, Ed. A. Hirsch, Series: Topics in Current Chemistry, Springer-Verlag, Berlin/Heidelberg, 1998, Vol. 199.
2 A. W. Jensen, S. R. Wilson and D. I. Schuster, *Bioorg. Med. Chem.*, 1996, **4**, 767.
3 M. Prato, *J. Mater. Chem.*, 1997, **7**, 1097.
4 C. S. Foote, *Top. Curr. Chem.*, 1994, **169**, 347.
5 (*a*) H. Imahori and Y. Sakata, *Adv. Mater.*, 1997, **9**, 537; (*b*) N. Martin, L. Sanchez, B. Illescas and I. Perez, *Chem. Rev.*, 1998, **98**, 2527; (*c*) J. F. Nierengarten, C. Schall and J. F. Nicoud, *Angew. Chem., Int. Ed. Engl.*, 1998, **37**, 1934; (*d*) M. Maggini, D. M. Guldi, S. Mondini, G. Scorrano, F. Paolucci, P. Ceroni and S. Roffia, *Chem. Eur. J.*, 1998, **4**, 1992; (*e*) E. Dietel, A. Hirsch, E. Eichhorn, A. Rieker, S. Hackbarth and B. Roder, *Chem. Commun.*, 1998, **21**, 1981; (*f*) D. M. Guldi, G. Torres Garcia and J. Mattay, *J. Phys. Chem.*, 1998, **102**, 9679; (*g*) S. Higashida, H. Imahori, T. Kaneda and Y. Sakata, *Chem. Lett.*, 1998, **7**, 605; (*h*) K. Tamaki, H. Imahori, Y. Nishimura, I. Yamazaki and Y. Sakata, *Chem. Commun.*, 1999, **7**, 625; (*i*) K. Tamaki, H. Imahori, Y. Nishimura, I. Yamazaki, A. Shimomura, T. Okada and Y. Sakata, *Chem. Lett.*, 1999, **3**, 227; (*j*) J. F. Nierengarten, J. F. Eckert, J. F. Nicoud, L. Ouali, V. Krasnikov and G. Hadziioannou, *Chem. Commun.*, 1999, **7**, 617; (*k*) N. Armaroli, F. Diederich, L. Echegoyen, T. Habicher, L. Flamigni, G. Marconi and J. F. Nierengarten, *New J. Chem.*, 1999, **23**, 77; (*l*) A. Polese, S. Mondini, A. Bianco, C. Toniolo, G. Scorrano, D. M. Guldi and M. Maggini, *J. Am. Chem. Soc.*, 1999, **121**, 3446; (*m*) P. Cheng, S. R. Wilson and D. I. Schuster, *Chem. Commun.*, 1999, **7**, 89; (*n*) T. Da-Ros, M. Prato, D. Guldi, E. Alessio, M. Ruzzi and L. Pasimeni, *Chem. Commun.*, 1999, **7**, 635; (*o*) S.-J. Liu, L. Shu, J. Rivera, H. Liu, J.-M. Raimundo, J. Roncali, A. Gorgues and L. Echegoyen, *J. Org. Chem.*, 1999, **64**, 4884.
6 N. S. Sariciftci, L. Smilowitz, A. J. Heeger and F. Wudl, *Science*, 1992, **258**, 1474.
7 The azothiophene chromophore was used, instead of the more conventional azobenzenes, mainly because aldehyde **1,** precursor to fulleropyrrolidine **2**, was readily available from BASF-AG (see Experimental section).
8 A. Hagfeldt and M. Grätzel, *Chem. Rev.*, 1995, **95**, 49.
9 P. Bonhôte, J.-E. Moser, R. Humphry-Baker, N. Vlachopoulos, S. M. Zakeeruddin, L. Walder and M. Grätzel, *J. Am. Chem. Soc.*, 1999, **121**, 1324.
10 C. Luo, C. Huang, L. Gan, D. Zhou, W. Xia, Q. Zhuang, Y. Zhao and Y. Huang, *J. Phys. Chem.*, 1996, **100**, 16 685.
11 G. Franco, J. Gehring, L. M. Peter, E. A. Ponomarev and I. Uhlendorf, *J. Phys. Chem. B*, 1999, **103**, 692.
12 A. Bianco, M. Maggini, G. Scorrano, C. Toniolo, G. Marconi, C. Villani and M. Prato, *J. Am. Chem. Soc.*, 1996, **118**, 4072.
13 D. Guldi, M. Maggini, G. Scorrano and M. Prato, *J. Am. Chem. Soc.*, 1997, **119**, 974.
14 M. Maggini, G. Scorrano and M. Prato, *J. Am. Chem. Soc.*, 1993, **115**, 9798.
15 M. K. Nazeeruddin, A. Kay, I. Rodicio, R. Humphry-Baker, E. Müller, P. Liska, N. Vlachopoulos and M. Grätzel, *J. Am. Chem. Soc.*, 1993, **115**, 6382.
16 J. C. Hummelen, B. Knight, J. Pavlovich, R. Gonzalez and F. Wudl, *Science*, 1995, **269**, 1554.
17 E. L. Yee, R. J. Cave, K. L. Guyer, P. D. Tyma and M. J. Weaver, *J. Am. Chem. Soc.*, 1979, **101**, 1131.
18 N. Vlachopoulos, P. Liska, J. Augunstinski and M. Grätzel, *J. Am. Chem. Soc.*, 1988, **110**, 1216.
19 M. Prato and M. Maggini, *Acc. Chem. Res.*, 1998, **31**, 519.
20 This assignment stems primarily from i) the larger potential separation between peak IV and its anodic counterpart relative to peaks I–III (230 mV *vs.* 90 mV) and V–VI, and ii) the analysis of peak IV characteristics upon variation of the scan rate (up to a scan rate of 100 V s^{-1}).
21 J. P. Stradins and V. T. Glezer, in *Encyclopedia of Electrochemistry of the Elements, Organic Section*, Ed. A. J. Bard and H. Lund, Marcel Dekker, Inc., New York, 1979, Vol. XIII, p. 163.
22 J. Roncali, *Chem. Rev.*, 1992, **92**, 711.
23 M. G. Hutchings, P. Gregory, J. S. Campbell, A. Strong, J.-P. Zamy, A. Lepre and A. Mills, *Chem. Eur. J.*, 1997, **3**, 1719.
24 The azobenzene moiety is known to undergo *trans–cis* isomerization. However, for the dye **3** no photochemical reaction was observed upon excitation both in the visible and in the UV spectral region.
25 The fluorescence spectrum of **2** at 77 K shows both the dye- and the fullerene-based emission.
26 The energy of the CS state (ΔG^0_{CS}) in CH_2Cl_2 was estimated using the dielectric continuum model. This model accounts for two spherical ions with radii R_A (C_{60}) and R_D (dye) separated by a distance R_{DA} immersed in a dielectric continuum with relative permittivity ε ($\varepsilon_{dichloromethane} = 8.93$). The center-to-center distance $R_{DA} = 11.8$ Å was obtained from PM3 semiempirical calculations. The standard potentials for oxidation [dye^+/dye] and reduction (C_{60}/C_{60}^-) processes in CH_2Cl_2, reported in Table 1, and E_{0-0} value of 1.97 eV relative to ^{1}dye* state were used in the calculations. (*a*) A. Z. Weller, *Phys. Chem. (Wiesbaden)*, 1982, **93**, 1982; (*b*) H. Imahori, K. Hagiwara, M. Aoki, T. Akiyama, S. Taniguchi, T. Okada, M. Shirakawa and Y. Sakata, *J. Am. Chem. Soc.*, 1996, **118**, 11 771; (*c*) S. I. van Dijk, C. P. Groen, F. Hartl, A. Brouwer and J. W. Verhoeven, *J. Am. Chem. Soc.*, 1996, **118**, 8425.
27 The spectral features of the charge-separated radical pair and the lifetime of the latter resembled those observed upon the dye excitation (535 nm).
28 Analogously, radiation-induced reduction of dyad **2** in toluene–propan-2-ol–acetone solution resulted in a distinct NIR absorption at 1010 nm.
29 Q. Xie, F. Arias and L. Echegoyen, *J. Am. Chem. Soc.*, 1993, **115**, 9818.
30 A. Wahl, M. Ulmann, A. Carroy, B. Jermann, M. Dolata, P. Kedzierzawski, C. Chatelain, A. Monnier and J. Augusynsky, *J. Electroanal. Chem.*, 1995, **396**, 41.
31 R. Dabestani, A. J. Bard, A. Campion, M. A. Fox, T. E. Mallouk, S. E. Webber and J. M. White, *J. Phys. Chem.*, 1988, **92**, 1872.
32 G. K. Boschloo and A. Goossens, *J. Phys. Chem.*, 1996, **100**, 19 489.

Paper 9/05287I